Assessing simulated arm lymphoedema by a prototype of bioimpedance spectroscopy device. Possible implication of its use in the follow up of patients who underwent extensive

ASSESSING SIMULATED ARM LYMPHOEDEMA BY A PROTOTYPE OF BIOIMPEDANCE SPECTROSCOPY DEVICE. POSSIBLE IMPLICATION OF ITS USE IN THE FOLLOW UP OF PATIENTS WHO UNDERWENT EXTENSIVE BREAST CANCER SURGERY

Velluzzi F[1], Corsale V[1], Tocco F[1], Dell'Osa AH[2], Fois A[3], Capone A[4], Marongiu G[4], Melis L[5], Serra C[6], Manuello Bertetto A[6], Concu A[7]

[1]Department of Medical Sciences and Public Health, University of Cagliari, Cagliari, Italy;
[2]Instituto de Desarrollo Economico e Innovación, Universidad Nacional de Tierra del Fuego, Antartida e Islas del Atlantico Sur, Ushuaia, Argentina;
[3]Biosignal Acquisition Systems Unit, Nomadyca Ltd., Kampala, Uganda;
[4]Orthopedic Clinic, Department of Surgical Sciences, University of Cagliari, Cagliari, Italy;
[5]Medical Faculty at the Bucarest Universitatea din Medicina si Farmacie Carol Davila, Bucarest, Romania;
[6]Department of Mechanics and Aerospace Engineering, Politecnico di Torino, Turin, Italy;
[7]2C Technologies Ltd., Academic Spin-Off at the University of Cagliari, Cagliari, Italy.

ABSTRACT

The aim of this research was to enable women after breast cancer surgery, in which arms lymphoedema often occurs, to self-monitor this disease using in-home an easy-to-use-device which assesses the arm's resistance ratio, considered an indirect, non-invasive index of increased extracellular water volume in those limbs. An homemade equipment based on the bioimpedance spectroscopy technique, was tested on 20 healthy volunteers which, by means of two ECG disposable electrodes, connected to the device both their dominant and auxiliary upper arms and changes in electrical resistance were assessed while an alternate current of low intensity and sweeping frequency from 15 to 75 kHz had be injected. In the same volunteers, an arm lymphoedema with about 100 ml excess of extracellular water was simulated by subtracting 0.8% from measured resistance values in each arm. The arms' resistance ratio against the increasing frequency gave rise to a parabolic branch visible on a mobile phone screen and, when the arm lymphoedema was simulated, the corresponding curve appeared positioned below that of the one without oedema. The patient's self-awareness, due to the device's self-management, could allow these subjects to actively approach the disease while sharing their results remotely with clinical specialists by an internet connection.

Keywords: Arm lymphoedema; Bioimpedance spectroscopy; Arm's electrical resistance; Remote control, IoT devices

1 INTRODUCTION

In women, lymphoedema of the upper limbs is a very frequent complication of axillary lymph nodes dissection in breast cancer surgery (BCS) because of the positivity of the sentinel lymph nodes biopsy. The arm on the side of the surgery becomes swollen due to an accumulation of lymphatic fluid in extracellular tissue, i.e. a protein-rich fluid, which could adversely affect the patient's quality of life [1].

Contact author: Alberto Concu
Address: Via Ravenna 24, I-09125 Cagliari, Italy
E-mail: aconcu44@gmail.com

In fact, in the affected arm (ALE) the lymphoedema gives rise to a restriction of movements as well as pain and reduced muscle strength together with joint stiffness [2, 3]. Because of these occurrences, ALE has also been studied with the aim of better understanding its effects on physical and mental health and quality of life [4, 10]. In a nursing study [11] which involved ten BCS women aged between 36 and 75 years who developed an ALE, patients spoke about the distress due to the lack of sensitivity and poor knowledge concerning lymphoedema manifested by several physicians, and the conflicting information that they obtained (as well as the difficulties in obtaining it) together with the lack and poor quality of specialized treatment centers. As confirmation of the importance of constant communication between patients and reference clinical structures, a very recent study [12] has shown that in a group of patients with ALE who underwent a training course aimed at their self-management of the state of the disease and rehabilitation activities to be carried out at home, quality of life was significantly better compared with that of the control group. The measurement of the electrical resistance of an arm having a lymphoedema has been used as an index inversely correlated to the degree of its clinical severity simply by comparing its resistance with that of the other arm by means of their arithmetical ratio [13 - 17]. Since it has been found that the resistance difference between an arm with lymphoedema and the other unaffected arm could reach no more than 10 Ω, or rather a very small difference considering that the corresponding increase in volume of the same affected limb could reach about 200 ml [17], it appears that some measurement errors can occur if the resistances of the two arms already show a difference before the ALE occurrence. In fact, due to its greater use, it has been found that in the dominant arm, the muscular masses may be more large than in the auxiliary one, so there is a greater volume of water in that dominant arm which also results in a physiological lower value of its electrical resistance [14, 15] [17 - 19].

More recently, Koelmeyer et al. [20] used bioimpedance spectroscopy (BIS) to test ALE in 20 patients in home care. Patients were given a package with a BIS commercial device together with lymphoedema education and support in promoting device's self-management, and carried out physical activity. Tests resulted in high adhesion of participants who felt more confident in using the BIS device, thus indicating a good prospective for home surveillance of ALE evolution by the patients themselves. Unfortunately, despite the increasing consensus for the use of BIS in measurements for the ALE patients, at present there are uncertainties about the real effectiveness of this technique as well as the availability of low-cost BIS devices that can be easily used by a large number of patients. In fact, in most of the previous studies, the tools used to monitor ALE were those designed for the measurement of body composition which implies a long lasting, multi-electrode arrangement to detect the bioimpedance values [21]. Moreover, these latter devices often have some preset frequencies of the injected current that can represent a limit of real clinical effectiveness for the ALE monitoring since, unlike devices in which a current with a sweep of increasing frequencies is applied (i.e. the BIS devices), there is uncertainty as to whether the measured resistance ratios of arms refers to a value with effective clinical importance. In any case, in several previous experiments the preset frequencies were of a very low value so that noise and distortions, that are typical of low frequency circuits, could occur in the acquisition of the electrical signals [22]. Furthermore, the devices used up to now were placed in the sales sector of high-cost biomedical equipment (several thousand Euros/$ USA), thus further limiting the possibility for the vast majority of patients with ALE of having personal BIS equipment for themselves. Thus, the possibility for them of obtaining a psychological benefit dependent on in-home self-assessment of their clinical condition is nullified.

Here we propose a very cheap electronic board (around € 50) as the motherboard to self-realize an inexpensive, easy-to-use, in-home device for ALE monitoring, with a highly reliable arm resistance ratio measurement. Moreover, this EIS equipment is an internet of things (IoT) tool as it is an interface between the biophysical and digital world [23], generating visual information on the evolution of this disease that the patient can effectively acquire on the display of a command and control device (i.e. smartphone, tablet), while, simultaneously, the same information is sent to an EIS specialized medical center via internet. Thanks to its intrinsic IoT device qualities, our tool can also be embedded in other different applications of medical areas.

2 METHODS

2.1 IOT EQUIPMENT

To acquire the arm resistance ratios we utilized a homemade prototype of BIS device that we easily built by utilizing the electronic board AD5933 (Analog Devices Inc., USA) which is a high precision impedance meter. The AD5933 generates a voltage signal with adjustable frequency up to 100 kHz with a resolution of 0.1 Hz. Recently, Noveletto et al. [24] developed some front end circuits to adapt the AD5933 impedance analyzer for use in BIS, and they concluded that the AD5933 could be suitable for biological applications in the frequency range of 5 to 100 kHz. What resulted was an IoT equipment for the arm resistance measurements, named ARM*sense*, which was housed in an aluminum case (6 x 12 x 22 cm) and weighed 450g. The ARM*sense* has been designed to operate not as a stand-alone device but, through a wireless connection, with a second device with Command and Control (*C&C*) functions. To facilitate domestic use, the ARM*sense* has been designed to operate in synergy with a mobile application (the ARM*sense* app) that can be used on smart phones and tablets equipped with an Android operating system and an active internet connection. The operating lifecycle of each session of the ARM*sense's* use is schematized in Figure 1. After the calibration phase has been successfully completed, the ARM*sense*'s microcontroller switches the input path from the calibration circuit to a circuit of electrodes. This is used to connect two disposable electrodes, applied to the upper arm of the patient under examination, to the device and the microcontroller subsequently starts the sampling session, performing a full frequency sweep. The frequency sweep is characterized by three fundamental configuration parameters, the lower frequency bound (L_{fb}), the upper

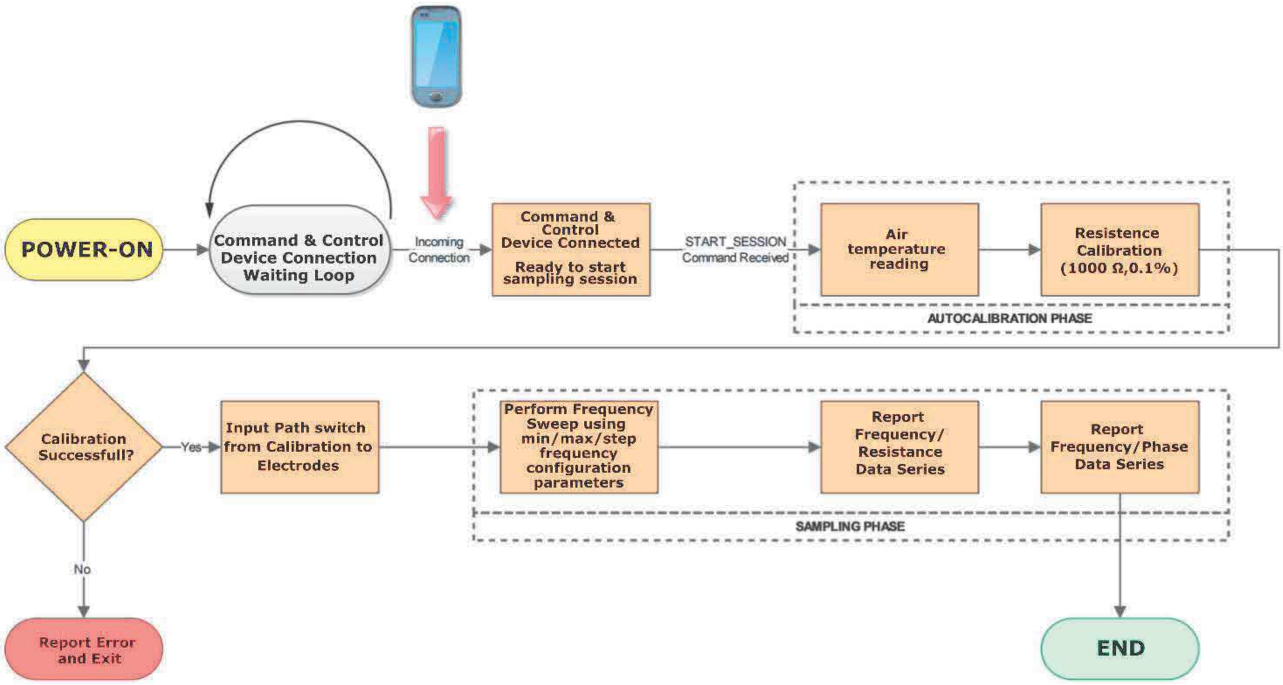

Figure 1 Block diagram schematizing the operating lifecycle of each session of the ARM*sense*

frequency bound (U_{fb}) and the frequency increment step (f_{step}). The number of resistance samples (S_n) acquired in each sampling session is a discrete value described by the equation:

$$S_n = \left[\left(U_{fb} - L_{fb}\right) \div f_{step}\right] \qquad (1)$$

As soon as the sampling phase is successfully completed, the ARM*sense*'s microcontroller transmits a vector to the C&C, consisting in S_n samples of resistance values acquired at each calculated frequency level between U_{fb} and L_{fb}, using an f_{step} increment.

The use of the ARM*sense* by patients was greatly simplified and speeded up thanks to the previously observed equivalence between the localized specific bioelectrical impedance of the arm and that of the total body [25], allowing the use of only two disposable electrodes attached to each upper arm (each electrode acts at the same time as injecting current and assessing resistance) to measure the resistance in these body segments of comfortably seated subjects. The electrical current injected along the arms of subjects had a constant voltage of 1.0 Vpp and the highest current value was of 0.25 mA, i.e. a typical condition of the short circuit to ground at V_{OUT}, therefore being absolutely harmless. Using a cut-off point of the arm resistance ratio to diagnose the onset of ALE was not favored as it represented a dimensionless image of this variable which therefore had little chance of capturing the patient's attention. Moreover, there is discordance in the numerical value of this important variable among papers concerned with defining it [13 - 17]. Therefore, we propose a regression curve generated by the upper arm resistance ratio values calculated as a function of the increasing frequency of the current injected into the arm. In this way, thanks to what appears on the screen of a mobile phone or a tablet, the patient at home is able to follow the course of the disease on the basis of simple comparisons between the shapes of these curves in the time elapsed since the onset of the ALE, simply by comparing the latest acquired upper arm resistance ratio curve with other previous ones extracted from the system memory on the same screen. These articulated two-dimensional images represent a more appealing way of mapping the progression of the illness of these patients.

2.2 SUBJECTS

The upper arm electrical resistance (R_{UA}) was assessed non-invasively in 20 healthy and voluntary right-handed young subjects (11 men and 9 women) by means of the ARM*sense*. Mean values of subject's age, weight and height were respectively: 28.4 ± 1.4 years, 63.8 ± 11.8 kg, 167.4 ± 7.5 cm and having a mean body mass index (BMI) of 22.8 ± 4.9 kg/m^2. The BIS measurement was made respecting the statements of the Helsinki declaration of 2000 and all the engaged subjects signed their informed consensus.

2.3 EXPERIMENTAL PROTOCOL

The BIS measurement was carried out partly at the Obesity section of Unit of Endocrinology and Metabolic Disease and partly at the Sports Medicine Unit of the Department of Medical Sciences and Public Health of the University of

Cagliari, in Italy, after obtaining the clinical history of each subject, and having acquired the patient's anthropometric measures.

Figure 2 Seated dummy of typical tested subjects is shown. The two red circles represent bipolar connection of the upper arm with the ARM*sense* equipment.

Two ECG disposable electrodes were easily placed by the subjects themselves at approximately the level of the upper and lower tendon-muscular junctions of the brachial biceps, respectively (see Figure 2). Subjects started their BIS measurements 5 minutes after the end of their preparation and, in any case, when they had the sensation that their upper body was as relaxed as possible. Each BIS measurement was repeated 3 times while the mean duration measurement for an electrode couple was about 20 s.

2.4 DATA ACQUISITION AND PROCESSING

We detected R_{UA} values of both dominant (R_d) and auxiliary (R_a) arms, starting from an injected current frequency of 15 kHz. This relatively high starting frequency was chosen in order to exclude the noise and distortions of the acquired electrical signals that can occur in low frequency circuits [22]. Then, both R_{UA} were subsequently detected at each step of frequency increments (f_{step}) of 15 kHz.

Acquired values of R_{UA} were processed up to having, for each upper arm, the subject's cumulative mean ± SD values at each f_{step}. Moreover, the mean ± SD values of R_d versus R_a ratios ($Ratio_{d/a}$) and vice versa ($Ratio_{a/d}$) were also calculated. The statistical method of regression, respectively for $Ratio_{d/a}$ and $Ratio_{a/d}$, mean values versus corresponding f_{step} values was also applied with the aim to graphically achieve two-dimensional representations of the R_{UA} versus f_{step} relationships in such a way to allow the patients to clearly visualize differences between the $Ratio_{d/a}$ and $Ratio_{a/d}$ respective trends. Two groups of BCS patients with an ALE of significant size, the one in the dominant arm ($R_{d,le}$) and the other in the auxiliary arm ($R_{a,le}$), were also simulated by reducing by 5 Ω the respective R_{UA} value really measured by the ARMsense at the f_{step} of 15 kHz and then reducing the values of R_{UA} measured at the other increasing f_{step} by the same percentage. On the basis of what observed by Smoot et al. [16], for each interested arm this R_{UA} fall might correspond to an increased extracellular water volume of about 100 ml. Subsequently, also the $R_{d,le}$ versus R_a ratios ($Ratio_{d,le/a}$) and vice versa ($Ratio_{a,le/d}$) were calculated, and the statistical method of regression, respectively for $Ratio_{d,le/a}$ and $Ratio_{a,le/d}$ mean values versus corresponding f_{step} values was also applied. The aim here was to produce graphic representations of the R_{UA} versus f_{step} relationships for the simulated ALE patients and to enable visual checking of the diagnostic potential of comparing different stages of this disease as, for instance, those of an arm at the time of diagnosed ALE and after a certain duration of the specific therapy administered to the patient. The statistical significance among data mean values and of the calculated regression equations was considered when $P<0.05$, and the MedCalc (Belgium) statistical package was chosen to investigate the data differences.

3 RESULTS

Anatomical measurements of the upper arms showed differences among the engaged subjects that were not statistically significant concerning the right versus left humerus bone length (28.6 ± 2.6 cm versus 28.7 ± 2.7 cm; P = 0.81) as well as the right versus left belly circumference of upper arms (27.5 ± 3.5 cm versus 27.6 ± 3.3 cm; P = 0.59). For this reason, it was not necessary to normalize acquired values of the R_{UA} regarding the morphological parameters of the upper arms. Table 1 shows that as the frequency of the injected current progressively increased both the dominant and auxiliary upper arm values of the R_{UA} progressively decreased. The table also shows that $Ratio_{d/a}$ increased and $Ratio_{a/d}$ decreased progressively with the increasing frequency of the injected current, together approaching the value of 1.0, since dominant and auxiliary R_{UA} values tended to be equal.

Table 1 - R_a: auxiliary arm; R_d: dominant arm; le: arm with simulated lymphoedema. Values are means ± SD.

Frequency (KHz)	Rd (Ω)	Ra (Ω)	Ratio d/a	Ratio d,le/a	Ratio a/d	Ratio a,le/d
15	631.7 ± 88.3	659.2 ± 88.5	0.958	0.951	1.043	1.043
30	550.3 ± 65.5	569.4 ± 85.4	0.968	0.959	1.035	1.035
45	525.8 ± 73.7	535.9 ± 80.4	0.981	0.973	1.019	1.019
60	518.3 ± 62.4	524.9 ± 72.3	0.987	0.981	1.013	1.013
75	516.3 ± 53.8	521.4 ± 64.7	0.990	0.982	1.001	1.001

However, the $Ratio_{d/a}$ values were always lower than the $Ratio_{a/d}$ ones. Both the simulated $Ratio_{d,le/a}$ and $Ratio_{a,le/d}$ mean values behaved similarly to the corresponding measured ones without ALE as the f_{step} increased.

Nevertheless, values of both $Ratio_{d,le/a}$ and $Ratio_{a,le/d}$ were always lower in comparison to those of $Ratio_{d/a}$ and $Ratio_{a/d}$ respectively. Equation (2) is the numerical representation, in terms of statistically significant quadratic regression (P=0.009), of the relationship of the $Ratio_{d/a}$, considered as the dependent variable, versus the f_{step}. Black colour curves and points in Figure 3 shows that the graphic function which represents what is numerically foreseen by equation (2), is an ascending branch of parabola with a progressive attenuation of the step $Ratio_{d/a}$ increments as the f_{step} rises.

$$ratio_{d\div a} = 0.94 + \left[+1.153 \times 10^{-3} \left(f_{step}\right)\right] - \left[0.7 \times 10^{-5} \left(f_{step}\right)^2\right] \quad (2)$$

The equation (3) concerns the numerical representation, in terms of statistically significant quadratic regression (P=0.025), of the relationship of the $Ratio_{d,le/a}$, considered as the dependent variable, versus the f_{step}, or when simulating in the former arm a lymphoedema due to an extracellular fluid increase of about 100ml.

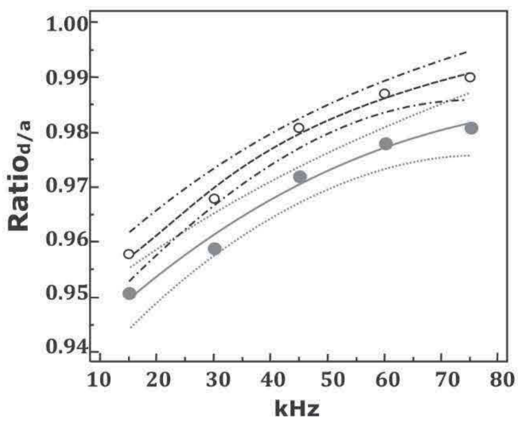

Figure 3 The branch of parabola concerning the $Ratio_{d/a}$ versus the f_{step} relationship is shown as a black dashed line with the 95% confidence interval and the empty circles are the relationship's measured values. The branch of parabola concerning the $Ratio_{d,le/a}$ versus the f_{step} relationship is shown as a grey continuous line with the 95% confidence interval and the full circles being the relationship's measured values.

Grey colour curves and points in Figure 3 show that the graphic function which represents what is numerically foreseen by equation (3) is still an ascending branch of parabola which also shows the progressive attenuation in increments of the step of dominant versus auxiliary arm ratio as the f_{step} rises.

$$ratio_{d,le\div a} = 9.93 + \left[+1.131 \times 10^{-3} \left(f_{step}\right)\right] - \left[0.63 \times 10^{-5} \left(f_{step}\right)^2\right] \quad (3)$$

However, the visual comparison of the two curves in Figure 3 highlights that the ascending segment of parabola having ordinate as $Ratio_{d,le/a}$ shows all values in this variable that are clearly lower than those homologues in the branch of parabola having $Ratio_{d/a}$ as ordinate.

Equation (4) is the numerical representation, in terms of statistically significant quadratic regression (P=0.025), of the relationship of the $Ratio_{a/d}$, considered as the dependent variable, versus the f_{step}.

Figure 4 shows that the graphic function which represents what is numerically foreseen by equation (3) is a descending branch of parabola with a progressive attenuation of the step $Ratio_{d/a}$ increments as the f_{step} rises.

$$ratio_{a\div d} = 1.06 + \left[-1.158 \times 10^{-3} \left(f_{step}\right)\right] + \left[0.63 \times 10^{-5} \left(f_{step}\right)^2\right] \quad (4)$$

Equation (5) concerns the numerical representation, in terms of statistically significant quadratic regression (P=0.028), of the relationship between auxiliary arm versus dominant arm ratio ($Ratio_{a,le/d}$) at each f_{step}, when simulating a reduction in the R_a due to about 100 ml of water accumulation in the extracellular fluid of these arms.

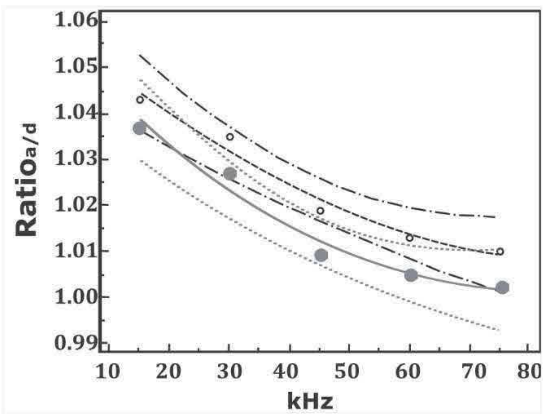

Figure 4. The branch of parabola concerning the $Ratio_{a/d}$ versus the f_{step} relationship is shown as a black dashed line with the 95% confidence interval and empty circles are the relationship's measured values. The branch of parabola concerning the $Ratio_{a,le/d}$ versus the f_{step} relationship is shown as a grey continuous line with the 95% confidence interval and full circles being the relationship's measured values.

$$ratio_{a,le\div d} = 1.058 + \left[-1.413 \times 10^{-3} \left(f_{step}\right)\right] + \left[0.89 \times 10^{-5} \left(f_{step}\right)^2\right] \quad (5)$$

Grey colour curves and circles in Figure 4 show that the graphic function which represents what is numerically foreseen by equation (5) is also a descending branch of parabola which shows the progressive attenuation of the step decrease of $Ratio_{a,le/d}$ as the f_{step} rises.
The visual comparison of the two curves in Figure 4 highlights that the branch of parabola having $Ratio_{a,le/d}$ as ordinate shows all values in this variable that are clearly lower than those having $Ratio_{a/d}$ as ordinate.

As soon as the ARM*sense* app is able to communicate via wireless connection with the ARM*sense* device, the BCS cooperation with the ARM*sense*'s microcontroller will automatically perform all the necessary steps to calibrate the device and to acquire the necessary resistance data.
After receiving those data, using the internet connection, the device sends them to a remote telemedicine central that processes the received data and immediately generates an output that is easily understood by the BCS user.

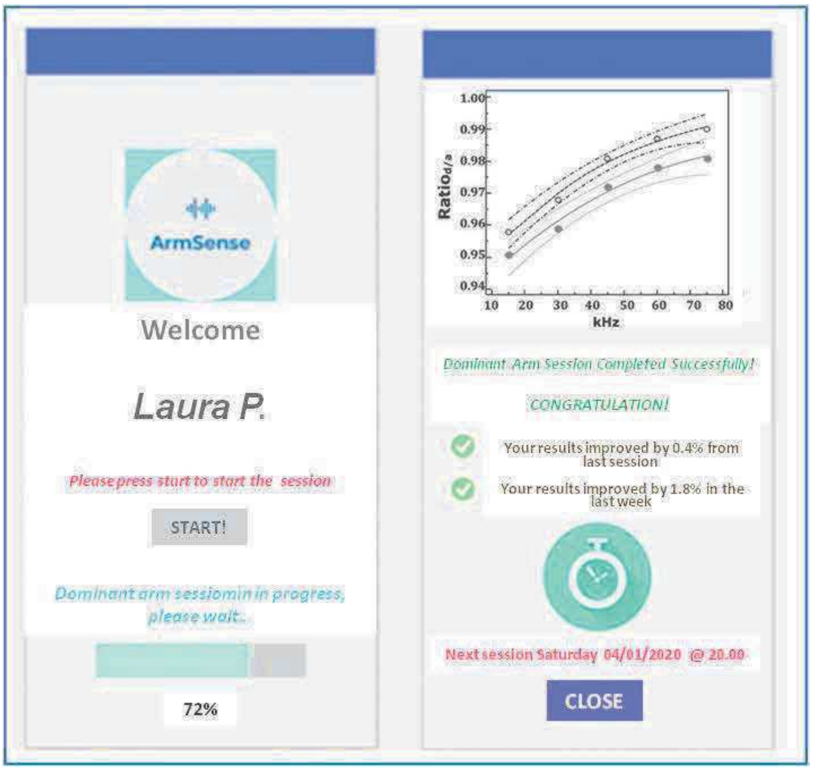

Figure 5 Representation, on an Android based smartphone, of two screens of the ARM*sense* application. On the left there is the main screen application and on the right is the screen with the Graphical User Interface (GUI) of the application.

The output of this process is visible in figure 5 on the right, in which the BCS patient's progress is well highlighted by the Graphical User Interface (GUI) of the application.
As an example, we inserted the graphs corresponding to that of Figure 3 and simulating, in given patient, two superimposed different interval of time concerning the ALE condition of a dominant arm: the one in which the ALE was manifest and the other when ALE had practically disappeared. In the GUI of Figure 5 some motivating phrases are presented that encourage the patient about her current ALE condition by comparing it both with the last session and the last week.

4 DISCUSSION

Experimental data acquired here showed an f_{step}-dependent progressive diminution in the assessed changes of the R_{UA} ratios between dominant versus auxiliary arm and vice versa, until the values of the two components of the relationships approached the same number. In fact, table 1 shows that when the f_{step} reached 75 kHz the $Ratio_{d/a}$ increased up to quasi 1 (i.e. 0.990) while the $Ratio_{a/d}$ reduced down to almost 1 (i.e. 1.001). These results agree with what is well known about the basis of the electrical properties applied to biological tissues [26]. In fact, with the progressive increase of the frequency of the current applied to the arms, the electrical capacities of cell membranes were practically short-circuited (they are discharged like when the positive pole is connected to the negative pole in a battery) so that the current passes easily through it, thus reducing the length of its path and therefore also the electrical resistance. Moreover, unlocking the current passages through the intracellular ionized fluid, several resistances resulted in parallel with those of the extracellular fluids giving rise to an equivalent resistance which, as expected from Ohm's law, progressively decreases as the current passes through the cells. This phenomenon affected both arms crossed by a high frequency alternating current. However, as previously observed in healthy subjects [19], the electrical resistance of the dominant arm still remained lower than that of the auxiliary one even if, for high frequency values, this difference in resistance between arms tended to be cancelled out. Nevertheless, when we simulated an ALE in the dominant arm the $R_{d,le}$ decreased as the simulated arm's excess of water volume increased, and this justifies the lower value of the $Ratio_{d,le/a}$ here observed with respect the $Ratio_{d/a}$ at each f_{step}.

Likewise, the same simulated lymphoedema affecting the auxiliary arm justifies the reduced values of the $Ratio_{a,le/d}$ with respect to the $Ratio_{a/d}$ at each f_{step}. Therefore, it appears evident that the ARM*sense* device allows us to discriminate between different stages of the ALE disease whether it concerns the dominant arm or the auxiliary arm. Nowadays, the current scenario of industrial innovations, called Industry 4.0 and implementing the Internet of Things array [27], has many applications in medical oncology clinical settings, both in the management of individual conditions and in the conditions of the patient cluster, including the ability to track and remotely monitor patients' progress by healthcare personnel as well as the possibility of improving patient self-management of chronic conditions. All of the above could contribute to optimizing early diagnosis in patients with ALE and therefore significantly improve their life conditions.

Finally, the ARM*sense* self-management could also reduce the risk of some mental suffering for these patients in that they become aware of their active contribution to improving their health condition. About this, a significant helping comes from the experimental observations of Carta et al. [28] which asserted that, in patients with major depression, a physical task consciously self-managed by the patient, "*may improve one's self-knowledge of physical well being*".

5 CONCLUSIONS AND IOT PERPECTIVES

The ARM*sense* App, which is installable and operable on Android based smartphones and tablets with an active internet connection, consents the BCS patient, when she wants, to start a sampling session by operating the "start!" button visible on the screen of a connected device. Subsequently, the ARM*sense*'s microcontroller will automatically acquire the upper arm resistance in the form of a geometric, quickly intuitive graphic displayed on the *C&C* screen from which it is easy to understand the actual state of the disease, by comparing the current critical data about the ALE with previous ones.

Thanks to its ability to evaluate the changes in water content of an organ, the ARM*sense* largely implements the characteristics of an IoT typical device.

In fact, besides for ALE patients, this device could also be of help in the self-assessment, in-home care of the edema status of people who have suffered fractures of the limbs where an extensive edema is established around the wound [29]. The orthopedic specialist can monitor the patient remotely and for prolonged periods of time also allowing him to participate more consciously in the progressive modulation of therapy with the help of the ARM*sense*, so benefitting also their psychological approach to their disease. Moreover, in obese patients with venous insufficiency where the self-performance of complex decongestive therapy based on compression, manual lymphatic drainage and remedial exercises has often been carried out at home [30], the possibility of having an ARM*sense* device at home remotely connected to the obesity Unit by internet to self-manage the trend of their limb swelling, among other clinical benefits could certainly contribute to reducing the risk of mental disorders that often occur in these patients [31], especially when it is associated with a controlled physical training [32]. Furthermore, it has been found that a fluid shift from blood vessels to interstitial tissue, facilitated by skeletal muscle damage, can occur in athletes engaged in extreme sports performances such as, for instance, those of ultra-endurance events [33] and, at present, there is little chance of predicting the trend of critical variables while competing [34, 35]. This interstitial fluid increase could now be assessed from a competing athlete by connecting one limb to a won ARM*sense* device which could inform both the athlete and the staff of sports doctors, who follow him remotely, about this skeletal muscle disorder. This latter facility keeps the athlete under constant medical and technical control in order to avoid both risks for his health and decreases in race performance and, reasonably, could also benefit the competing athlete's mood by increasing his will to win the race also thanks to a highlight cardiovascular performance due to a post-synaptic facilitation from both brain-mental and limb-reflex information convergence to the heart nervous control center in the brain stem [36].

6 STUDY LIMITATIONS

A possible limitation of this study might be ascribed to the fact that BCS patients having an ALE were all simulated by extrapolating information from a previous paper in which a robust relationship was shown between the excess water volume in an arm affected by lymphoedema and its electrical resistance [17]. However, studies in which diseases concerning the behaviour of body fluids contents were totally simulated by mathematically modelling discrete parts of the fluid container are by now considered indispensable for the understanding of even very complex physio-pathological phenomena [37, 38]. Nevertheless, all this does not exclude the need to reproduce this experimentation on patients suffering from ALE as soon as possible.

ABBREVIATION GLOSSARY

ALE: Arm lymphoedema.
ARM*sense*: homemade device name.
BCS: Breast Cancer Surgery.
BIS: Bioimpedance Spectroscopy.
C&C: Command and Control device.
ECG: Electrocardiography.
f_{step}: frequency increment.
GUI: Graphical User Interface.
IoT: Internet of Things.
L_{fb}: Lower frequency bound.
R_a: resistance values of auxiliary arm.
$R_{a,le}$: resistance values of auxiliary arm with simulated lymphoedema.
$Ratio_{a/d}$: Ratio between R_a and R_d.
$Ratio_{a,le/d}$: Ratio between $R_{a,le}$ and R_d.
R_d: resistance values of dominant arm.
$Ratio_{d/a}$: Ratio between R_d and R_a.
$R_{d,le}$: resistance values of dominant arm with simulated lymphedema.
$Ratio_{d,le/a}$: Ratio between $R_{d,le}$ and R_a.
R_{UA}: resistance values of upper arms.
S_n: Number of resistance samples.
U_{fp}: Upper frequency bound.
V_{OUT}: Output voltage.
V_{pp}: Voltage peak to peak.

REFERENCES

[1] McWayne J. and Heine S.P., Psychologic and social sequelae of secondary lymphedema: a review. *Cancer*, Vol. 104, No. 3, pp. 457-466, 2005.

[2] Schrenk P., Hochreiner G., Fridrik M. and Wayand W., Sentinel node biopsy performed before preoperative chemotherapy for axillary lymph node staging in breast cancer. *Breast J.*, Vol. 9, pp. 282–287, 2003.

[3] Rietman J.S., Dijkstra P.U., Geertzen J.H.B., Baas, P., de Vries J., Dolsma W.V., Groothoff J.W., Eisma W.H. and Hoekstra H.J., Treatment-related upper limb morbidity 1 year after sentinel lymph node biopsy or axillary lymph node dissection for stage I or II breast cancer. *Ann. Surg. Oncol.*, Vol. 11, pp. 1018–1024, 2004.

[4] Oliveri J.M., Day J.M., Alfano C.M., Herndon J.E., Katz M.L., Bittoni M.A., Donohue K and Paskett E.D., Arm/hand swelling and perceived functioning among breast cancer survivors 12 years post-diagnosis: CALGB 79804. *J. Cancer Surviv.*, Vol. 2, No. 4, pp. 233-242, 2008.

[5] Morgan P.A., Franks P.J. and Moffatt C.J., Health-related quality of life with lymphoedema: a review of the literature. *Int. Wound J.*, Vol. 2, No. 1, pp. 47-62, 2005.

[6] Tobin M.B., Hubert J.L., Meyer L. and Mortimer P.S., The psychological morbidity of breast cancer-related arm swelling. *Cancer*, Vol. 72, No. 11, pp. 324-352, 1993.

[7] Beaulac S.M., McNair L.A., Scott T.E., La Morte W.W. and Kavanah M.T., Lymphoedema and quality of life in survivors of early-stage breast cancer. *Arch. Surg.*, Vol. 137, No. 11, pp. 1253-1257, 2002.

[8] Pereira de Godoy J.M., Braile D.M., de Fatima Goday M. and Longo O. Jr., Quality of life and peripheral lymphoedema. *Lymphology*, Vol. 35 No. 2, pp. 72-75, 2002.

[9] Moffatt C.J., Franks P.J., Doherty D.C., Williams A.F., Badger C., Jeffs E., Bosanquet N. and Mortimer P.S., Lymphoedema: an underestimated health problem. *Q. J. Med.*, Vol. 96, No. 10, pp. 731-738, 2003.

[10] Passik S., Newman M., Brennan M. and Holland J., Psychiatric consultation for women undergoing rehabilitation for upper-extremity lymphedema following breast cancer treatment. *J. Pain Symptom. Manage.*, Vol. 8, No. 4, pp. 226-233, 1993.

[11] Carter B.J., Women's experiences of lymphoedema. *Oncol. Nurs. Forum.*, Vol. 24 No. 5, pp. 875-882, 1997.

[12] Omidi Z., Kheirkhah M., Abolghasemi J. and Haghighat S., Effect of lymphedema self-management group-based education compared with social network-based education on quality of life and fear of cancer recurrence in women with breast cancer: a randomized controlled clinical trial. *Qual. Life Res.*, Vol. 29, No. 7, pp. 1789-1800, 2020.

[13] Cornish B.H., Bunce I.H., Ward L.C., Jones L.C. and Thomas B.J., Bioelectrical impedance for monitoring the efficacy of lymphoedema treatment programmes. *Breast Cancer Res. Treat.*, Vol. 38, pp. 169-176, 1996.

[14] Warren A.G., Janz B.A., Slavin S.A. and Borud L.J., The use of bioimpedance analysis to evaluate lymphedema, *Ann. Plast. Surg.*, Vol. 58, pp. 541–543, 2007.

[15] Ward L.C., Dylke E., Czerniec S., Isenring E. and Kilbreath S.L., Confirmation of the reference impedance ratios used for assessment of breast cancer-related lymphedema by bioelectrical impedance spectroscopy. *Lymphat. Res. Biol.*, Vol. 9 No. 1, pp. 47-51, 2011.

[16] Smoot B., Zerzan S., Krasnoff J., Wong J., Cho M. and Dodd M., Upper extremity bioimpedance before and after treadmill testing in women post breast cancer treatment, *Breast Cancer Res. Treat.*, Vol. 148, pp. 445–453, 2014.

[17] Jung M., Jeon J.Y., Yun G.J, Yang S., Kwon S. and Seo Y.J., Reference values of bioelectrical impedance analysis for detecting breast cancer-related lymphedema. *Medicine* (Baltimore), Vol. 97, No. 44, pp. e12945, 2018.

[18] Lim S.M., Han Y., Kim S.I. and Park H.S., Utilization of bioelectrical impedance analysis for detection of lymphedema in breast Cancer survivors: a prospective cross sectional study. *BMC Cancer*, Vol. 19, 2019.

[19] Dell'Osa A.H., Gel M., Concu A., Fois A., Mela Q., Loviselli A. and Velluzzi F., Electrical Impedance Spectroscopy of right and left upper arms in healthy subjects: a non-invasive method for easy monitoring of structural changes in limbs? *Proceedings of the 17th International Conference on the Electrical Bioimpedance*, Joinville, Brazil, Bertemes-Filho P. Ed.: ICEBI 2019, IFMBE Proceedings, Vol. 72, pp. 216-220, 2020.

[20] Koelmeyer L.A., Moloney E., Boyages J., Sherman K.A. and Dean C.M., Prospective surveillance model in the home for breast cancer-related lymphoedema: a feasibility study. *Breast Cancer Res. Treat.*, Vol. 1, pp. 1-12, 2020.

[21] Salazar G., Leyton B., Aguirre C. Anziani A., Weisstaub G. and Corvalán, C., Anthropometric and bioimpedance equations for fat and fat-free mass in chilean children 7-9 years of age. *Br .J. Nutr.*, Vol. 8, pp. 1-6, 2020.

[22] Bucci D., Introduction to noise analysis in low frequency circuits, *Analog electronics for measuring systems*, Bucci D. Ed., ISTE ltd: London, UK, pp. 121–152, 2017.

[23] Tan L. and Wang N, Future internet: The Internet of Things. *Proceedings of the 3rd International Conference on Advanced Computer Theory and Engineering (ICACTE),* Chengdu, China, Vol. 5, pp. V5-376-V5-380, 2010.

[24] Noveletto F., Bertemes-Filho P. and Dutra D., Analog Front-End for the Integrated Circuit AD5933 used in Electrical Bioimpedance Measurements. *Book of 2° Latin American Conference on Bioimpedance,* Montevideo, Uruguay, pp. 48–51, 2016.

[25] Mereu E., Succa V., Buffa R., Sanna. C., Mereu R.M., Catte O. and Marini, E., Total body and arm bioimpedance in patients with Alzheimer's disease. *Exp. Gerontol.*, Vol. 102, pp. 145-148, 2018.

[26] Ivorra A., Bioimpedance monitoring for physicians: an overview. *Cent, Nac, Microelectron Biomed. Appl. Gr.* Vol. 1, pp. 1-35, 2002.

[27] Kelly J.T., Campbell K.L., Gong E. and Scuffham P., The Internet of Things: Impact and Implications for Health Care Delivery. *J. Med. Internet Res.*, Vol. 22 No. 11, pp. e20135, 2020.

[28] Carta M.G., Hardoy M.C., Pilu A., Sorba M., Floris A.L., Mannu F.A., Baum A., Cappai A., Velluti C. and Salvi M., Improving physical quality of life with group physical activity in the adjunctive treatment of major depressive disorder. *Clin. Pract. Epidemiol. Ment. Health*, Vol. 4, pp. 1-6, 2008.

[29] Lim S.K. and Lim J.Y., Phase angle as a predictor of functional outcomes in patients undergoing in-hospital rehabilitation after hip fracture surgery. *Arch. Gerontol. Geriatr.*, Vol. 89, No. 104060, 2020.

[30] Gradalski T. and Ochalek K., Lay Caregivers Education in Multicomponent Compression Bandaging in Obese Patients with Lower Limb Edema: A Case–Control Pilot Study. *Lymphat. Res. Biol.*, Vol. 18, No. 5, pp. 428-432, 2020.

[31] Pinna F., Sardu C., Orrù W.,Velluzzi F., Loviselli A., Contu P. and Carpiniello B., Psychopathology, psychosocial factors and obesity. *Rivista di Psichiatria.* Vol. 51, No. 1, pp. 30-36, 2016.

[32] Velluzzi F., Tocco F., Deledda A., Ghiani G. and Concu A., Training impulses: A method to quantify exercise intensity in postmenopausal obese women. *Proceedings of the 2016 IEEE International Symposium on Medical Measurements and Applications,* Benevento, Italy, pp. 481-486, 2016.

[33] Weitkunat T., Knechtle B., Knechtle P., Rüst C.A. and Rosemann T., Body composition and hydration status changes in male and female open-water swimmers during an ultra-endurance event. *J. Sports Sci.*, Vol. 30, No. 10, pp. 1003-1013, 2012.

[34] Marongiu E., Crisafulli A., Pinna M., Ghiani G., Degortes N., Concu A. and Tocco F., Evaluation of reliability of field tests to predict performance during Ironman Triathlon. *Sport Sci. Health*, Vol. 9, pp. 65–71, 2013.

[35] Wu W.C., Concu A., Solinas R., Fois A., Loviselli A., Deledda A. and Velluzzi F., Metabolic power and energy cost of mechanical work carried out by a sailor engaged in a solo ocean race: a case study. *Int. J. Mechanics and Control*, Vol. 19, pp.19-32, 2018.

[36] Tocco F., Crisafulli A., Milia R., Marongiu E., Mura R., Roberto S., Todde F., Concu D., Melis S., Velluzzi F., Loviselli A., Concu A. and Melis F., Nervous facilitation in cardiodynamic response of exercising athletes to superimposed mental tasks: Implications in depressive disorder. *Clin. Pract. Epidemiol. Ment. Health*, Vol. 11, No. 1, pp. 166–173, 2015.

[37] Niccolini G., Manuello A., Capone A., Marongiu G., Dell'Osa A.H., Fois A., Velluzzi, F. and Concu, A., Possible Assessment of Calf Venous Pump Efficiency by Computational Fluid Dynamics Approach. *Front. Physiol. Comput. Physiol and Medicine*, Vol. 11, No.1003, 2020.

[38] Behbahani M., Behr M., Hormes M., Steinseifer U., Arora D., Coronado O. and Pasquali M., A review of computational fluid dynamics analysis of blood pumps. *Eur. J. Appl. Math.,* Vol. 20, pp. 363–397, 2009.